Improved irreversibility behavior and critical current density in MgB_2-diamond nanocomposites

Y. Zhao[a] and C. H. Cheng
School of Materials Science and Engineering, University of New South Wales, Sydney 2052, NSW, Australia and State Key Lab for Mesophysics, Department of Physics, Peking University, Beijing 100871, China

X. F. Rui and H. Zhang
State Key Lab for Mesophysics, Department of Physics, Peking University, Beijing 100871, China

P. Munroe
School of Materials Science and Engineering, University of New South Wales, Sydney 2052, NSW, Australia

H. M. Zeng
Key Laboratory of Polymeric Composites and Functional Materials, The Ministry of Education, Zhongshan University, Guangzhou, 510275, People's Republic of China

N. Koshizuka and M. Murakami
Superconductivity Research Laboratory, ISTEC, 1-10 13 Shinonome, Koto-ku, Tokyo, 135-0062, Japan

(Received 10 February 2003; accepted 8 July 2003)

MgB_2-diamond nanocomposite superconductors have been synthesized by addition of nanodiamond powder. Microstructural analysis shows that the nanocomposite superconductor consists of tightly packed MgB_2 nanograins (~50–100 nm) with highly dispersed and uniformly distributed diamond nanoparticles (~10–20 nm) inside the grains. The J_c-H and $H_{\mathrm{iir}}-T$ characteristics have been significantly improved in this MgB_2-diamond nanocomposite, compared to MgB_2 bulk materials prepared by other techniques. Also, the J_c value of 1×10^4 A/cm^2 at 20 K and 4 T and the H_{irr} value of 6.4 T at 20 K have been achieved. © *2003 American Institute of Physics.*
[DOI: 10.1063/1.1606884]

Since the discovery of superconductivity at 39 K in MgB_2,[1] significant progress has been made in improving the performance of MgB_2 materials.[2–4] MgB_2 offers the possibility of wide engineering applications in the temperature range 20–30 K, where conventional superconductors, such as Nb_3Sn and Nb–Ti alloy, cannot play any roles due to their low T_c. However, the realization of large-scale applications for MgB_2-based superconductivity technology essentially relies on the improvement of the pinning behavior of MgB_2 in high fields. As it has poor grain connection and a lack of pinning centers, MgB_2 often exhibits a rapid decrease in critical current density, J_c, in high magnetic fields. Fortunately, through the formation of nanoparticle structures in bulk MgB_2[2–4] and thin films,[5] the problem of the poor grain connection can be solved, and the flux pinning force can also be significantly enhanced due to an increase of pinning centers served by grain boundaries. In order to improve further the performance of MgB_2, it is necessary to introduce more pinning centers, especially those consisting of nanosized second-phase inclusions, which often provide strong pinning forces.

Nanodiamond, prepared by the detonation technique, has been widely used as an additive to improve the performance of various materials.[6] Yet, nanodiamond has never been used to increase the flux pinning force in MgB_2 superconductors until the present study. The high dispersibility of the nanodiamond powder makes it possible to form a high density of nanoinclusions in MgB_2 matrix. In this letter, we have prepared the MgB_2-diamond nanocomposite, which consists of tightly packed MgB_2 nanograins (~50–100 nm) with diamond nanoparticles (~10–20 nm) wrapped within the grains. This unique microstructure provides the composite with a good grain connection for the MgB_2 phase and a high density of flux-pinning centers served by the diamond nanoparticles. Compared to the MgB_2 bulk materials prepared with other techniques, the irreversibility line has been significantly improved and the J_c in high magnetic fields has been largely increased in the MgB_2-diamond nanocomposite.

The MgB_2-diamond nanocomposites with compositions of $MgB_{2-x}C_x$ ($x=0\%$, 5%, 8%, and 10%) were prepared by solid-state reaction at ambient pressure. Mg powder (99% purity, 325 meshes), amorphous B powder (99% purity, submicron-size), and nanodiamond powder (10–20 nm) were mixed and ground in air for 1 h. An extra 2% of Mg powder was added in the starting materials to compensate the loss of Mg caused by high temperature evaporation. The mixed powders were pressed into pellets with dimensions of 20 $\times10\times3$ mm^3 under a pressure of 800 kg/cm^2, sandwiched into two MgO plates, sintered in flowing Ar at 800 °C for 2 h, and then quenched to room temperature in air. In order to compare the substitution effect of carbon in boron in MgB_2 with the additional effect of the nanodiamond in MgB_2, a sample with an added 1.5 wt % of nanodiamond in MgB_2 was prepared. The sintering temperature and the sintering time for this sample were reduced respectively to 730 °C and 30 min in order to reduce the chemical reaction between the

[a]Electronic mail: y.zhao@unsw.edu.au

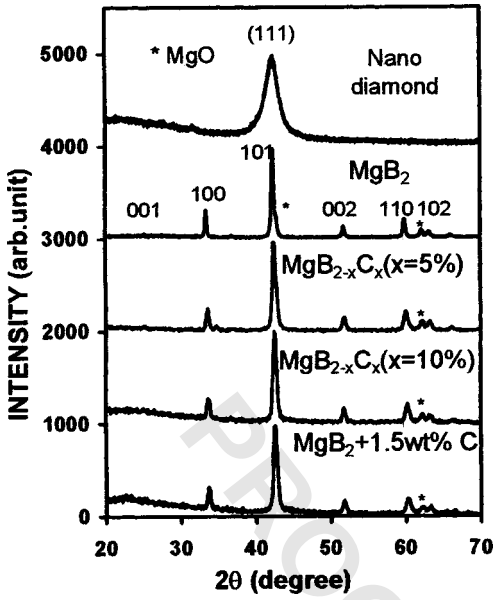

FIG. 1. Powder XRD patterns for MgB_2-diamond nanocomposites. The pattern on the top row is for the nanodiamond.

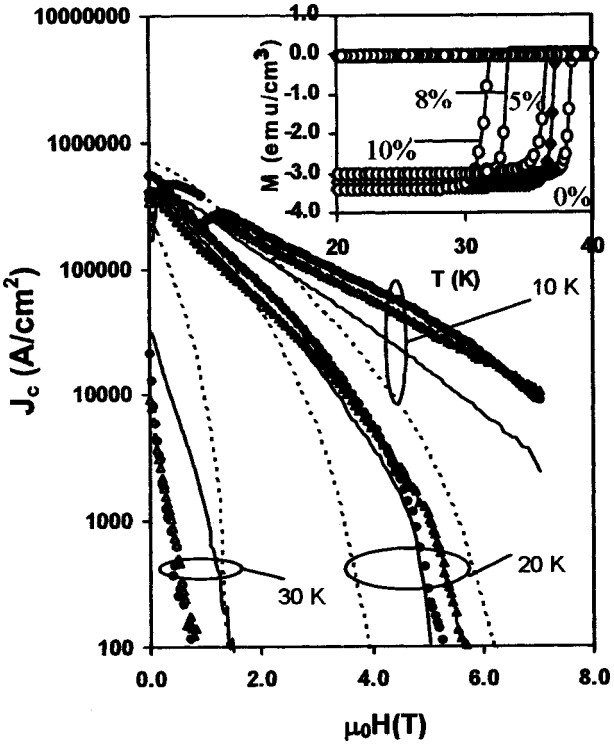

FIG. 2. Magnetic field dependence of J_c at 10, 20, and 30 K for $MgB_{2-x}C_x$ with $x=0\%$ (dashed lines), 5% (solid lines), 8% (solid circles), and 10% (opened triangles). Inset: superconducting transition curves for the diamond-doped samples. The closed circles represent the results for the sample 1.5 wt % C.

MgB_2 and the diamond. This sample has been referred to as 1.5 wt % C.

The crystal structure was investigated by powder x-ray diffraction (XRD) using an X'pert MRD diffractometer with Cu $K\alpha$ radiation. The microstructure was analyzed with a Philips CM200 field emission gun transmission electron microscope (FEGTEM). Dc magnetization measurements were performed in a superconducting quantum interference device (Quantum Design MPMS-7). J_c values were deduced from hysteresis loops using the Bean model. The sample's dimensions with typical values of $0.7\times2.1\times2.7$ mm^3 are used in the calculation of J_c. The values of the irreversibility field, H_{irr}, were determined from the closure of hysteresis loops with a criterion of 10^2 A/cm^2.

Figure 1 shows the XRD patterns of the nanodiamond powder and the typical MgB_2-diamond composites. The reflection (111) of the diamond is extremely broad and an amorphous-phase-like background can be seen in the XRD pattern. The particle size of the nanodiamond powder is estimated to be about 20 nm according to the width of the reflection. In relation to the MgB_2-diamond composites, one of the impurity phases is MgO, which may have formed during the mixing of raw materials in air. Diamond should be present as another impurity phase in the composites however, its main reflection (111) cannot be seen in XRD patterns, due to an overlap with the MgB_2 (101) peak. As for the sample with the low doping level of $x=5\%$, its XRD pattern looks the same as that of the undoped MgB_2, except for a decrease of the lattice parameter along the a axis, indicating that a certain amount of carbon atoms have substituted for boron atoms in MgB_2. This result is consistent with those reported by other groups, which show that partial substitution of boron by carbon results in a decrease of the lattice parameter.[7,8] With increasing doping level, an amorphous-phase-like background in the XRD pattern gradually appears, suggesting the existence of unreacted nanodiamond in the sample. As for the diamond added MgB_2 sample (1.5 wt % C), which contains an $x=5.4\%$ equivalent percentage of carbon atoms, the background of its XRD pattern shows some similarity to the background of the nanodiamond, suggesting that a substantial amount of unreacted nanodiamond exists within this sample.

The substitution of boron by carbon in our MgB_2 can also be reflected by the gradual decrease of T_c with increasing carbon content (see the inset of Fig. 2). The values of onset T_c for these carbon-substituted MgB_2 samples are 38.6 K for $x=0\%$, 36.1 K for $x=5\%$, 33.0 K for $x=8\%$, and 31.3 K for $x=10\%$. The T_c for the sample 1.5 wt % C is 36.9 K, which is higher than that for the sample of $x=5\%$ ($T_c=36.1$ K), despite the former having a higher equivalent atomic percentage of carbon ($x=5.4\%$).

Figure 2 shows the magnetic field dependence of J_c at 10, 20, and 30 K for the carbon-substituted MgB_2 samples. At 30 K, the undoped MgB_2 exhibits the highest J_c and the slowest decrease of J_c with H; whereas the sample of $x=10\%$ shows the lowest J_c and the quickest drop of J_c with H. It is evident that the J_c-H behavior at 30 K for these samples is positively correlated to their T_c values. However, when the temperature decreases to the values far below T_c, a totally different situation appears. For example, at 10 and 20 K, the diamond-doped samples show a much better J_c-H behavior. The J_c drops much more slowly in diamond-doped samples than in pure MgB_2. The best J_c at 20 K is found in the sample of $x=10\%$, reaching a value of 6×10^3 A/cm^2 in a 4 T field, indicating that a strong flux pinning force exists in these diamond doped samples.

The $H_{\mathrm{irr}}-T$ relations for the diamond-substituted MgB_2 are shown in the inset of Fig. 3. The $H_{\mathrm{irr}}(T)$ curves get steeper with increasing doping level. The best value of H_{irr}

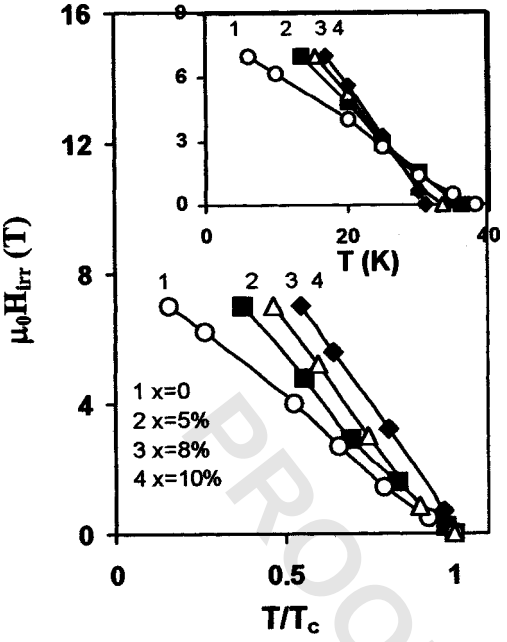

FIG. 3. Variation of H_{irr} with reduced temperature T/T_c for $MgB_{2-x}C_x$ with $x=0\%$, 5%, 8%, and 10%. Inset: $H_{irr}-T$ plot for the same data shown in the main figure.

reaches 5.7 T at 20 K for the sample of $x=10\%$. As the T_c values vary with the diamond-doping level, only the $H_{irr}-T$ relation cannot directly reflect the intrinsic irreversibility behavior for the samples of different doping levels. In the main panel of Fig. 3, the temperature dependence of H_{irr} is replotted using a reduced temperature, T/T_c. It is evident that the irreversibility field shifts towards higher temperatures with the increase of the diamond-doping level. The result clearly shows that the diamond doping does enhance the flux pinning in MgB_2 significantly.

However, the effect of diamond doping on the enhancement of flux pinning in MgB_2 may be counterbalanced by its suppression on superconductivity, as clearly shown in the situation of $T=30$ K (see Fig. 2). This counterbalancing effect may also exist at other temperatures, even when the effect of the J_c enhancement is dominant. The further increase of J_c depends critically on reducing the T_c-suppression effect in the MgB_2-diamond composite. This idea is confirmed by the results obtained in the diamond-added sample, 1.5 wt % C, which has a higher T_c than other diamond-doped samples (see inset of Fig. 2) and contains more nanodiamond inclusions as suggested by the XRD analysis (see Fig. 1) and confirmed by our transmission electron microscopy analysis shown later. As shown in Fig. 4, the diamond-added sample shows a much better J_c-H behavior than the carbon-substituted sample. Its J_c reaches 1×10^4 A/cm^2 at 20 K and 4 T, and its H_{irr} reach 6.4 T at 20 K. In fact, at all temperatures below 35 K, the J_c-H behavior (results at 20 K are shown here only) and the $H_{irr}-T$ relation (see the inset of Fig. 4) of the diamond-added sample are much better than those of other samples in this study.

Figure 5 shows the typical results from microstructural analysis for the diamond-substituted MgB_2 and diamond-

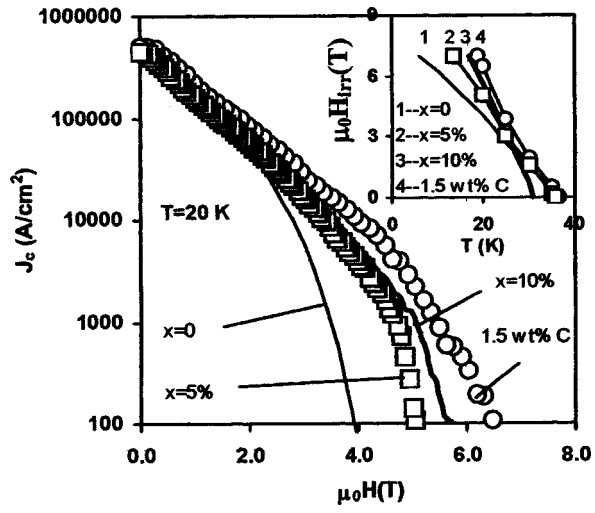

FIG. 4. Comparison of J_c-H relations at 20 K for diamond-added MgB_2 sample 1.5 wt % C with diamond-substituted MgB_2. The atomic percentages of carbon in the sample 1.5 wt % C and the sample of $x=5\%$ are almost the same. Inset: $H_{irr}-T$ relations for the same samples shown in the main figure.

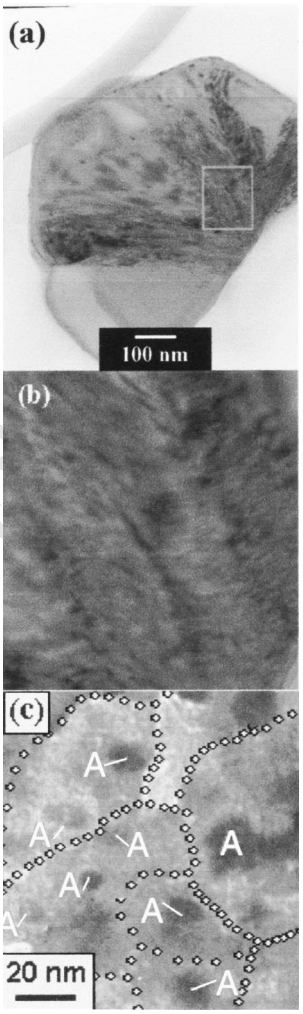

FIG. 5. FEGTEM micrographs for (a) a typical grain (~1 μm) of diamond substituted MgB_2 with $x=5\%$ which shows the high density of dislocations (dark stripes) in the sample; (b) an enlarged view of the dislocations in Fig. 5(a); (c) diamond added MgB_2 with the carbon content of 1.5 wt %. The grain boundaries of MgB_2 are indicated by the guidelines. The diamond nanoparticles are marked by letter *A* beside it (for small ones) or on the particles (for big ones). The atomic percentages of carbon in these two samples are almost the same.

added MgB_2 samples. The diamond-substitutional sample mainly consists of relatively large MgB_2 grains (~ 1 μm or so in size) with a high density of dislocations. In some areas, discrete nanosized particles can be seen [Figs. 5(a) and 5(b)]. The diamond-added sample mainly consists of two kinds of nanoparticles: MgB_2 grains with a size of 50–100 nm and diamond particles with a size of 10–20 nm [see Fig. 5(c)]. In fact, this diamond-added MgB_2 forms a typical nanocomposite material. The nanodiamond particles are inserted into the MgB_2 grains. As the ab plane coherence length of MgB_2 is about 6–7 nm,[9] these 10–20 nm-sized diamond inclusions, with a high density, are ideal flux pinning centres and are responsible for the high performance in our samples.

The significant improvement of J_c and H_{irr} in the nanodiamond-added samples (1.5 wt %) can be attributed to their nanocomposite structure which consists of two kinds of nanoparticles: MgB_2 grains with a size of 50–100 nm and diamond particles with a size of 10–20 nm. The enhanced number of grain boundaries associated with the smaller grain size can enhance the flux pinning, as reported previously.[2–5] However, only this factor cannot fully explain the experimental results because the enhancement of flux pinning in the nanodiamond-added samples (1.5 wt %) is even much better than that in the Ti-doped MgB_2[2–4] where the average grain size of MgB_2 reaches 8–10 nm. This indicates that there may be other mechanisms of flux pinning enhancement in the present system. One of the most likely candidates is the diamond nanoparticles which may play a similar role as Y_2O_3 nanoparticles did in Y_2O_3-doped MgB_2.[10] It is worth noting that, compared to the Y_2O_3 Y_2O_3-doped MgB_2 the nanodiamond-added samples (1.5 wt %) has a higher J_c and H_{irr}. This may be due to the advantage of the nanodiamond whose lattice contact (for the cubic diamond $a=0.356$ nm) is very close to the c axis of MgB_2 ($c=0.352$ nm). Therefore, these diamond nanoparticles may provide nucleation centres for MgB_2 and are tightly bound to them. It has been reported that some undoped MgB_2 samples with a slight grain texture also show a high J_c and H_{irr} (see, for example, Narozhnyi *et al.*),[11] suggesting that achieving a textured microstructure is another effective way to improve J_c of MgB_2 because of a slight anisotropy existing in this system. Accordingly, it is expected that the performance of the MgB_2-diamond nanocomposite may be further improved by optimizing the microstructure and the doping levels.

In summary, we have synthesized a MgB_2-diamond nanocomposite superconductor by adding nanodiamond powder into MgB_2. The nanocomposite consists of tightly packed MgB_2 nanograins ($\sim$50–100 nm) with diamond nanoparticles ($\sim$10–20 nm) inserted inside these grains. The J_c-H and $H_{irr}-T$ characteristics have been significantly improved in this MgB_2-diamond nanocomposite, in comparison with MgB_2 bulk materials prepared with other techniques.

The authors are grateful to Sisi Zhao for her helpful discussion in preparing the manuscript. This work was supported in part by the University of New South Wales (Goldstar Award for Cheng). Financial support from the Ministry of Science and Technology of China (NKBRSF-G19990646) is also acknowledged.

[1] J. Nagamatsu, N. Nakagawa, T. Muranaka, Y. Zenitani, and J. Akimitsu, Nature (London) **410**, 63 (2001).
[2] Y. Zhao, Y. Feng, C. H. Cheng, L. Zhou, Y. Wu, T. Machi, Y. Fudamoto, N. Koshizuka, and M. Murakami, Appl. Phys. Lett. **79**, 1154 (2001).
[3] Y. Zhao, D. X. Huang, Y. Feng, C. H. Cheng, T. Machi, N. Koshizuka, and M. Murakami, Appl. Phys. Lett. **80**, 1640 (2002).
[4] Y. Zhao, Y. Feng, T. Machi, C. H. Cheng, D. X. Huang, Y. Fudamoto, N. Koshizuka, and M. Murakami, Europhys. Lett. **57**, 437 (2002).
[5] C. B. Eorn, M. K. Lee, J. H. Choi, L. J. Belenky, X. Song, L. D. Cooley, M. T. Maus, S. Patnaik, J. Jiang, M. Rikel, A. Polyanskii, A. Gurevich, X. Y. Cai, S. D. Bu, S. E. Babcock, E. E. Hellstrom, D. C. Larbalestier, N. Rogado, K. A. Regan, M. A. Hayward, T. He, J. S. Slusky, K. Inumaru, M. K. Haas, and R. J. Cava, Nature (London) **411**, 558 (2001).
[6] Q. Chen and S. Yun, Mater. Res. Bull. **35**, 1915 (2000).
[7] T. Takenobu, T. Ito, D. H. Chi, K. Prassides, and Y. Iwasa, Phys. Rev. B **64**, 134513 (2001).
[8] W. Mickelson, J. Cumings, W. Q. Han, and A. Zettl, Phys. Rev. B **65**, 052505 (2002).
[9] M. Xu, H. Kitazawa, Y. Takano, J. Ye, K. Nishida, H. Abe, A. Matsushita, N. Tsujii, and G. Kido, Appl. Phys. Lett. **79**, 2779 (2001).
[10] J. Wang, Y. Bugoslavsky, A. Berenov, L. Cowey, A. D. Caplin, L. F. Cohen, J. L. MacManus Driscoll, L. D. Cooley, X. Song, and D. C. Larbalestier, Appl. Phys. Lett. **81**, 2026 (2002).
[11] V. N. Narozhnyi, G. Fucks, A. Handstein, A. Gumbel, J. Eckert, K. Nenkov, D. Hinz, O. Gutfleisch, A. Walte, L. N. Bogacheva, I. E. Kostyleva, K.-H. Muller, and L. Schultz, cond-mat/0206513.